NOx removal efficiency and ammonia selectivity during the NOx storage-reduction process over Pt/BaO(Fe, Mn, Ce)/Al2O3 model catalysts. Part II: Influence of Ce and Mn-Ce addition

N. Le Phuc, X. Courtois, F. Can, S. Royer, P. Marecot, D. Duprez

Applied Catalysis B: Environmental 102 (2011) 362–371.
DOI: 10.1016/j.apcatb.2010.12.043

NOx removal efficiency and ammonia selectivity during the NOx storage-reduction process over Pt/BaO(Fe, Mn, Ce)/Al_2O_3 model catalysts.

Part II: influence of Ce and Mn-Ce addition

N. Le Phuc, X. Courtois*, F. Can, S. Royer, P. Marecot, D. Duprez

Laboratoire de Catalyse en Chimie Organique, Université de Poitiers, UMR6503 CNRS,

40 Av. Recteur Pineau, Poitiers, 86022, France

*Corresponding author: E-mail: xavier.courtois@univ-poitiers.fr

Abstract

It was previously demonstrated in the first part of this work that NOx storage-reduction process over Pt/BaO/Al_2O_3 model catalyst is limited by the reduction step, with ammonia emission since H_2 is not fully consumed. The stored NOx react preferentially with the introduced H_2 giving NH_3, than with NH_3 in order to produce N_2. Mn addition favors the NOx reduction with ammonia leading to better conversion and selectivity, but only at 400°C. In part II, a special attention was focused on the role of Ce and Mn-Ce addition in regard to the NOx conversion and the ammonia emission in the 200-400°C temperature range. With ceria modified Pt/20Ba/Al catalyst, significant improvements are obtained from 300°C. In addition to the enhancement of the NOx+NH_3 reaction, the ammonia selectivity is maintained at a lower level compared with Pt/Ba(Mn)/Al catalysts, even in the case of a large H_2 excess. It is attributed to the ammonia oxidation into N_2 via the available oxygen at the catalyst surface. A synergetic effect is observed between Mn and Ce when they are added simultaneously in Pt/Ba/Al catalyst.

Keywords : NOx storage; NOx reduction; ammonia; barium; lean/rich cycles; manganese; ceria.

1. Introduction

NOx storage reduction (NSR) catalysts are a possible way to reduce NOx for diesel and lean burn engines [1]. They work mainly in lean condition. During these periods, NOx are oxidized over precious metals and stored on basic compounds such as barium oxides, mainly as nitrates. Periodically, the catalyst is submitted to short periods for few seconds in rich conditions in order to reduce the trapped NOx into N_2 [2,3]. In addition with deactivation by sulfur poisoning [4,5] and thermal aging [6,7,8], another problem can be the NOx reduction selectivity. Indeed, in addition to N_2O, NH_3 emission can be observed [9,10]. This work is mainly focused on this ammonia emission. In the first part of this study [11], NOx removal efficiency of Pt/Ba/Al model catalyst was studied using lean/reach cycling condition with H_2 as reducer and CO_2 and H_2O in the feed stream. It was established that the NOx reduction selectivity strongly depends on the hydrogen conversion which was introduced in the rich pulses: NH_3 is emitted since hydrogen is not fully converted, whatever the NOx conversion rate. Moreover, the ammonia selectivity increases with the amount of unconverted hydrogen. This study has showed that Pt/Ba/Al catalyst is able to reduce NOx into N_2 using NH_3 as reducer, but the ammonia formation rate via the NOx reduction by H_2 is higher than the ammonia reaction rate with NOx to form N_2. It was also showed that H_2O inhibits the ammonia formation because it limits the formation of CO via the reverse WGS reaction, CO being a precursor for the isocyanate formation, which leads to ammonia after hydrolysis. In absence of other introduced C-compounds, CO_2 also favors the ammonia formation via the isocyanate route, with intermediate formation of CO via the reverse WGS reaction.

Then, the influence of iron and manganese, both commonly proposed in NSR formulation, was studied. Fe is reported to improve the catalyst sulfur resistance because it leads to the inhibition of bulk barium sulfates formation [12,13]. Fe is also reported to be active in NOx SCR by ammonia [14]. However, we showed that Fe addition leads to a strong catalyst deactivation after successive tests, probably due to interaction between iron and platinum. Mn can also participate to the NOx storage [15,16] and is active for the NOx reduction by NH_3 [14,17,18,]. In fact, we found that Mn addition induces different behaviors depending on the temperature test. At low temperature (200-300°C), Mn is a poison for the reduction step. By contrast, at 400°C, Mn favors the NOx reduction with ammonia, even if the introduced hydrogen is not fully converted, leading to a significant enhancement of the NOx conversion and N_2 selectivity. However, if a large hydrogen excess is introduced, the ammonia selectivity becomes very close with Pt/20Ba/Al and Pt/20BaMn/Al. Thus, the NOx conversion can be improved but the low

temperature activity is still a problem. In this second part, influences of Ce and Ce-Mn addition were studied, especially toward ammonia emission. Cerium compounds are well known in automotive catalysis for their oxygen storage/release behavior [19]. However, some interesting cerium properties were put in evidence for NOx-trap systems. Ceria is claimed to improve the barium stability, with an inhibiting effect for the barium aluminate formation [20]. Barium-cerium interaction was evidenced by $BaCeO_3$ formation even if this specie is decomposed under NO_2-H_2O and destabilized under CO_2 [8]. Migration of Ba ions through CeZrOx compound was also observed by Liotta et al. [21] in Pt-CeZrOx/Ba-Al_2O_3 catalyst. This Ba-Ce interaction could allow a better control of the Ba dispersion as well as an improvement of the resistance to SO_2 poisoning [22]. These interesting properties toward sulfur poisoning regeneration are attributed to lower cerium sulfates stability compared with barium sulfates [23,24]. In addition, ceria compounds are able to store NOx [25,26,21]. For example, Ba/CeO_2 material has exhibited a higher NOx storage efficiency than Ba/Al_2O_3 in the 200-400°C temperature range [20]. Similar results were obtained by Lin et al. [27] who investigated the effect of La or Ce addition on the NOx storage properties of Pt/Ba-Al_2O_3. The low temperature efficiency of ceria based storage material was also demonstrated with MnOx-CeO_2 oxide [28]. Besides, cerium addition could improve the NOx removal efficiency. Indeed, Pt/MgO-CeO_2 catalyst was found to be active for low-temperature NO SCR by H_2 of NO [29]. Concerning the ammonia selectivity, cerium could lead to lower emission. Indeed, in a recent work about the NOx storage reduction (NSR) behavior of Pt/$Ce_xZr_{1-x}O_2$ catalysts, it was observed that the ammonia selectivity decreases with the increase of the cerium loading [30]. Thus, the aim of the present work is to examine the influence of Ce addition on the NSR efficiency of Pt/Ba/Al model catalyst, with a special attention for the ammonia emission. Furthermore, association of Mn and Ce addition is also studied.

2. Experimental

2.1. Catalysts preparation

The detailed preparation protocols are reported in part I [11]. The reference catalyst contains 1wt% Pt and 20wt% BaO supported on alumina. Alumina powder (230 $m^2.g^{-1}$) was immersed in an ammonia solution and was firstly impregnated using a barium nitrate salt. After evaporation at 80°C and drying at 120°C, the obtained powder was treated at 700°C under synthetic dry air. Platinum was then impregnated using a $Pt(NH_3)_2(NO_2)_2$ aqueous solution.

After drying, the catalyst was pre-treated at 700°C for 4h under N_2, and finally stabilized at 700°C for 4h under a mixture containing 10% O_2, 5% H_2O in N_2.

The modified samples were prepared using the same protocol except that the nitrate salts of Mn^{IV} and Ce^{III} were simultaneously added with the barium salt. In this case, a part of alumina was replaced to assure the desired "additive/Ba" molar ratio. For the cerium modified samples, Ce/Ba molar ratio was varied between 0.25 and 2. In addition, catalysts containing both Mn and Ce were also prepared. In this case, Mn/Ba molar ratio is always 1 (7.2wt% for Mn) and Ce is added with Ce/Ba molar ratio between 0.1 and 1. The Ce and Mn-Ce modified catalysts are noted Pt/20BaCeX/Al and Pt/20BaMnCeX/Al, respectively, X being the Ce/Ba molar ratio.

2.2. Catalyst characterizations

2.2.1. Specific surface measurement

The BET surface areas and pore volumes were deduced from N_2 adsorption-desorption at -196°C carried out with a Tristar 3000 Micromeritics apparatus. Prior to the measurement, the samples were treated at 250°C under vacuum for 8 h to eliminate the adsorbed species.

2.2.2. Platinum dispersion measurement

The platinum dispersion was determined using the H_2 chemisorption method. The catalyst was first reduced under pure hydrogen at 500 °C for 1 h and then flushed at the same temperature under argon for 3 h. The reactor was cooled down to -85°C for Ce and Mn containing catalysts. Hydrogen was then dosed on the sample until saturation. After flushing under argon for 10 min, the sample was exposed to hydrogen again. The amount of chemisorbed hydrogen was taken as the difference between the two hydrogen exposures.

2.2.3. XRD analysis

X-ray powder diffraction was performed at room temperature with a Bruker D5005 apparatus using a Kα Cu radiation (λ=1.54056 Å). The powder was deposited on a silicon monocrystal sample holder. The crystalline phases were identified by comparison with the ICDD database files.

2.2.4. Temperature programmed reduction (TPR)

Prior to the TPR test, the catalyst (50 mg) was first pretreated in situ under oxygen at 300°C for 30 min and cooled to room temperature. After flushing under argon for 45 min, the reduction

was carried out from room temperature up to 800°C under a 1%H_2/Ar mixture, using a 5°C min^{-1} heating rate. The sample was maintained at 800°C for 30 min before cooling under argon. The hydrogen consumption was followed by thermal conductivity.

2.2.5. Oxygen storage capacity (OSC)

The OSC was measured at 400°C under atmospheric pressure. The sample (5 mg) was continuously purged with helium (30 mL min^{-1}). Alternate pulses (0.265 mL) of pure O_2 and pure CO were injected every 2 min [31]. The oxygen storage capacity (OSC) was calculated from the CO consumption after stabilization.

2.3. Catalytic activity measurements

2.3.1. NOx storage capacity (NSC) measurement

The same protocol as described in Part I [11] was used in this study. The catalyst (60mg) was first was pretreated in situ for 30 min at 550°C, under a 10% O_2, 10% H_2O, 10% CO_2 and N_2 mixture (total flow rate: 10 L h^{-1}), and then cooled down to the storage temperature under the same mixture. The sample was then submitted to a lean mixture as reported in Table 1, at 200°C, 300°C and 400°C. Both NO and NOx concentrations (NO+NO_2) were followed by chemiluminescence. H_2O was removed prior to NOx analysis with a membrane dryer. The NOx storage capacity was estimated by the integration of the recorded profile for the first 60 seconds and the contribution of the reactor volume was subtracted. With the conditions used in this test, 57.4 µmol NOx per gram of catalyst were injected in 60s, which corresponds to the lean period durations of the NSR test in cycling conditions. Results are expressed as the NIOx storage rate (%) for 60s. In addition, the catalyst oxidation activity was estimated as the NO_2/NOx ratio (%) at saturation (usually about 900s).

Table 1: Rich and lean gas compositions used for the NOx conversion test (60s lean / 3s rich). Total flow rate: 10 L h^{-1}.

Gas	NO	H_2	O_2	CO_2	H_2O	N_2
Rich	-	1 to 6 %	-	10 %	1 0%	Balance
Lean	500 ppm	-	10 %	10 %	10 %	Balance

2.3.2. NOx conversion in cycling conditions

Before measurement, the catalyst (60mg) was treated in situ at 450°C under 3% H_2, 10% H_2O, 10% CO_2 and N_2 for 15 min. The sample was then cooled down to the desired temperature (200, 300 and 400°C) under the same mixture. The NOx conversion was studied in cycling condition by alternatively switching between lean (60s) and rich (3s) conditions using electro-valves. The gas composition is described in Table 1. NO and NO_2 were followed by chemiluminescence, N_2O by specific FTIR, H_2 by mass spectrometry. Before the analyzers, H_2O was trapped in a condenser at 0°C. As described in part I [11], the trapped water was analyzed by two different HPLC for NH_4^+, NO_2^- and NO_3^-. NO_2^- and NO_3^- were added to the unconverted NOx. The N_2 selectivity is calculated assuming no other N-compounds than NO, NO_2, N_2O, NH_3. Some tests were also performed using a Multigas FTIR detector (MKS 2030) without water trap system. Same results were then obtained.

3. Results

3.1. BET, XRD and platinum dispersion.

The BET specific surface areas of the studied samples are reported in Table 2. Compared with the Pt/20Ba/Al reference catalyst (127 m^2g^{-1}), addition of cerium leads to a continuous decrease of the specific surface areas, down to 65 m^2g^{-1} for Pt/20BaCe2/Al. It can be attributed to the partial alumina substitution by ceria which should have a lower specific surface. A decrease of the pore volume is also observed, especially for Ce/Ba molar ratio higher than 0.75. The same trend is observed with Pt/20BaMnCeX/Al catalysts. Mn addition to Pt/20Ba/Al leads to a small decrease of the BET surface area from 127 to 118 m^2g^{-1}. Supplementary addition of cerium induces a more significant area loss, especially for Ce/Ba molar ratios equal to 0.5 and 1. It also corresponds to a significant drop in the pore volume.

XRD patterns of the Pt/20BaCeX/Al catalysts are reported in Figure 1. The main detected crystalline phases are $BaCO_3$, $BaAl_2O_4$ and CeO_2. The intensities of the ceria diffraction peaks increase with the ceria loading, but the particle sizes can not be reasonably estimated with the Scherrer equation since an enlargement of the main peak is caused by the presence of $BaAl_2O_4$ ($2\theta=32°$). The diffraction peaks of $BaAl_2O_4$ decrease with cerium loading, which is consistent with the decrease of the alumina loading. $BaCO_3$ is observed only for Ce/Ba molar ratio 0.75 and higher. It suggests that the barium dispersion decreases with the cerium additions, which is consistent with the related BET specific surface areas losses. For the catalysts containing both

Mn and Ce, the only detected phase containing Mn is $BaMnO_3$ (Figure 2). CeO_2 is detected only for the samples with the higher Ce loadings: Pt20BaMnCe0,5 and Pt20BaMnCe1. As for Pt/20BaCeX/Al samples, it also corresponds with a decrease of the $BaAl_2O_4$ diffraction peaks.

Table 2: Catalysts composition, corresponding BET surface areas and pore volumes. $(Mn/Ba)_{molar\ ratio} = 1$ in Pt/20BaMnCeX/Al catalysts.

catalyst	Ce/Ba molar ratio	Ce loading (wt %)	BET surface area (m^2g^{-1})	Pore volume (cm^3g^{-1})
Pt/20Ba/Al	-	-	127	0.36
Pt/20BaCe0.25/Al	0.25	4.6	119	0.31
Pt/20BaCe0.5/Al	0.50	9.1	109	0.30
Pt/20BaCe0.75/Al	0.75	13.7	92	0.29
Pt/20BaCe1/Al	1.00	18.3	80	0.22
Pt/20BaCe1.5/Al	1.50	27.4	72	0.18
Pt/20BaCe2/Al	2.00	36.5	65	0.15
Pt/20BaMn/Al	-	-	118	0.29
Pt/20BaMnCe0.1/Al	0.10	1.8	112	0.29
Pt/20BaMnCe0.2/Al	0.20	3.7	109	0.28
Pt/20BaMnCe0.5/Al	0.50	9.1	89	0.25
Pt/20BaMnCe1/Al	1.00	18.3	78	0.21

Concerning the platinum dispersion, Shinjoh et all have clearly demonstrated that platinum particles are better anchored on ceria-based materials, compared with alumina support, due to strong Pt-O-Ce bonds [32]. Then, a better platinum dispersion can be expected with the increase of the ceria loading. However, at the same time, a decrease of the BET surface area is also observed (Table 2). Finally, after the thermal treatments at 700°C, no evidence of a significant change of the platinum dispersion is observed depending on the Mn and/or Ce loading. It reaches around 10% for all studied samples.

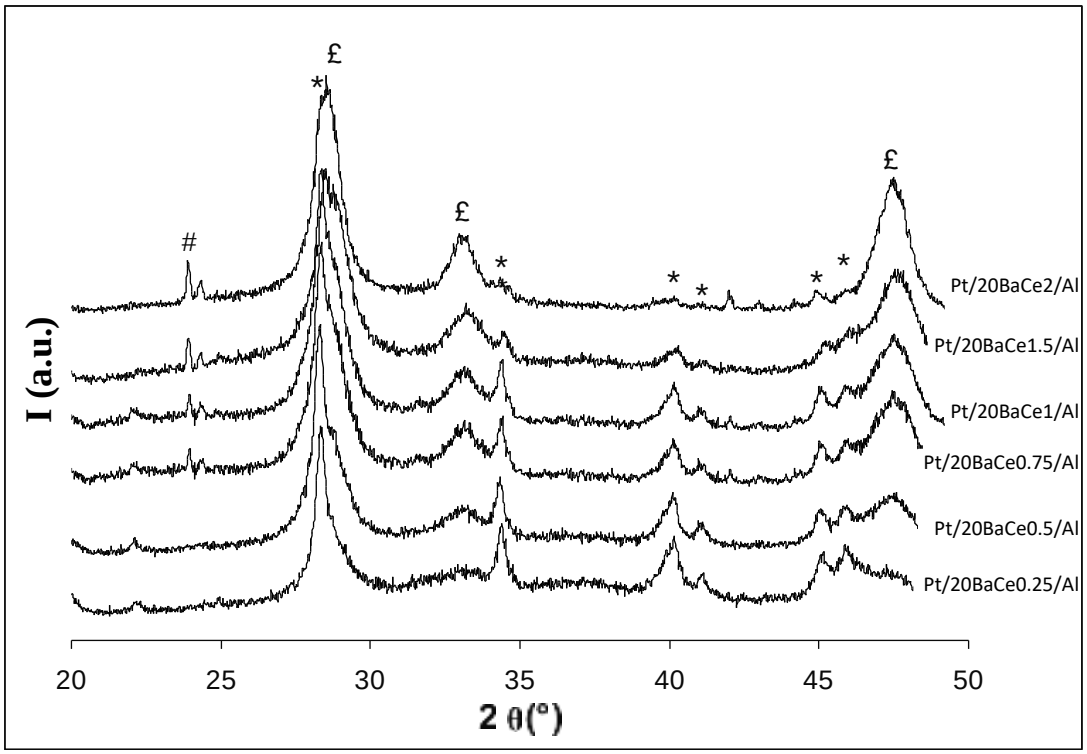

Figure 1: X ray diffractogramms of Pt/20BaCeX/Al catalysts.
(#) $BaCO_3$, (*) $BaAl_2O_4$, (£) CeO_2.

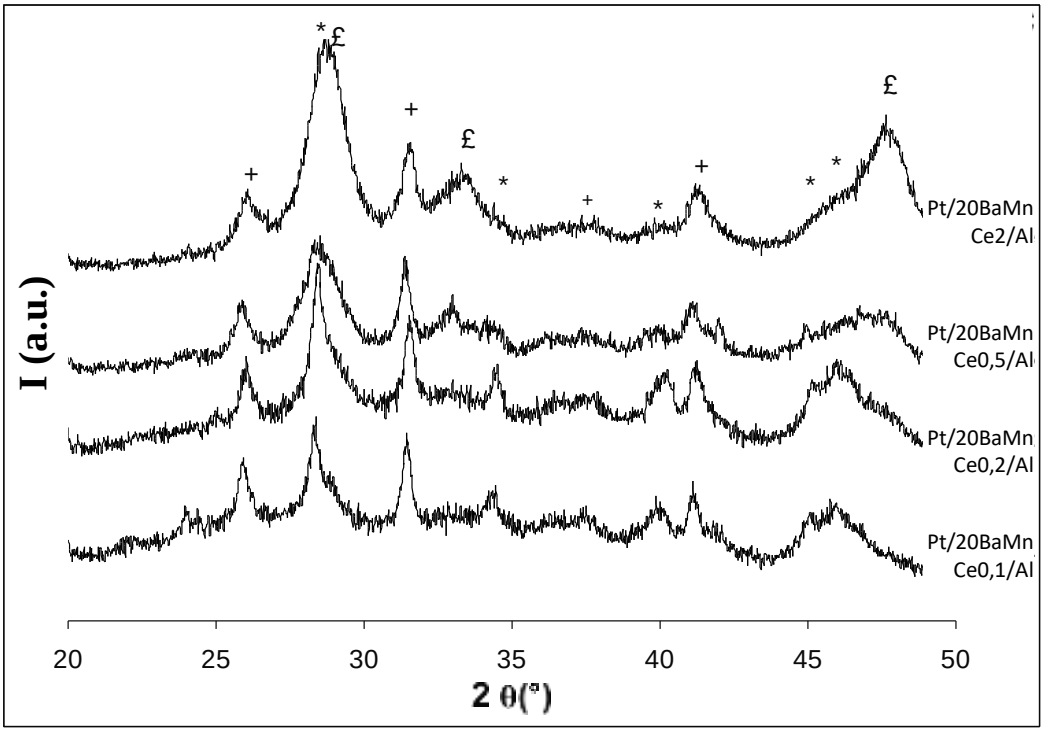

Figure 2: X ray diffractogramms of Pt/20BaMnCeX/Al catalysts.
(*) $BaAl_2O_4$, (+) $BaMnO_3$, (£) CeO_2.

3.2. NOx storage capacity

Influences of Ce or Mn-Ce additives on Pt/20Ba/Al on the NOx storage rate for 60s were investigated at 200, 300 and 400°C. For the Pt/20BaCeX/Al catalysts, results reported in Table 3 show that an optimal composition is observed with Pt20BaCe0.75. However, the obtained storage rate is close to the one obtained with the Pt/20Ba/Al reference catalyst, but the BET surface area of the Ce modified sample is 30% lower. In fact, ceria is known to be able to store NOx, but ceria addition also induces a BET surface loss. Indeed, for the higher Ce loading, the BET surface loss is not balanced by the ceria storage behavior.

Table 3: NOx storage rate (%) for 60s and NO_2/NOx ratio at saturation (between brackets). Catalyst weight: 60mg ; total NOx storage corresponds to 57.4 $\mu mol_{NOx}/g$ in 60s.

Catalyst	NOx storage rate for 60s (%) and (NO_2/NOx ratio at saturation (%))		
Temperature (°C)	200°C	300°C	400°C
Pt/20Ba/Al	57 (16)	73 (24)	83 (37)
Pt/20BaCe0.25/Al	52 (15)	71 (27)	82 (42)
Pt/20BaCe0.5/Al	60 (21)	68 (28)	76 (40)
Pt/20BaCe0.75/Al	63 (13)	73 (20)	79 (35)
Pt/20BaCe1/Al	58 (15)	70 (25)	79 (36)
Pt/20BaCe1.5/Al	53 (14)	62 (24)	76 (38)
Pt/20BaCe2/Al	47 (21)	57 (27)	70 (39)
Pt/20BaMn/Al	61 (14)	74 (21)	84 (38)
Pt/20BaMnCe0.1/Al	63 (16)	73 (22)	86 (40)
Pt/20BaMnCe0.2/Al	63 (16)	77 (21)	93 (44)
Pt/20BaMnCe0.5/Al	67 (13)	81 (21)	96 (41)
Pt/20BaMnCe1/Al	78 (13)	93 (24)	99 (43)

The influence of cerium addition in Pt/20BaMn/Al catalysts was also examined. Some storage improvements were obtained depending on the cerium loading and the temperature test. At 200°C, a moderate storage improvement is observed for $(Ce/Ba)_{\text{molar ratio}} \leq 0.5$, whereas the NOx storage rate is significantly better with the Pt/20BaMnCe1/Al. It reaches 78% versus 57% for the Pt/20Ba/Al reference catalyst. At 300 and 400°C, the influence of the cerium loading becomes significant from $(Ce/Ba)_{\text{molar ratio}} = 0.2$, and increases with the cerium loading even if the BET surface areas decrease. The maximum storage rates, obtained with Pt/20BaMnCe1/Al,

are 93 and 99%, respectively. Finally, Mn or Ce addition does not improve the storage rate for 60s, but a beneficial effect is observed when Ce and Mn are added together. In this case, the more the temperature is low, the higher cerium loading is needed.

Table 3 also reports the NO_2/NOx ratios measured at saturation. The influence of the cerium loading is rather limited compared with the influence of the temperature test. Generally, the cerium addition is rather negative at 200°C, there is nearly no influence at 300°C, and a small beneficial effect is observed at 400°C. However, after saturation, the NOx storage capacity of the catalysts varies as follow: Pt/20BaMnCe1/Al >> Pt/20BaCe1/Al > Pt/20BaMn/Al > Pt/20Ba/Al. Then, the significant enhancement of the NOx storage rate for 60s when Ce and Mn are added together can not be attributed to an improvement of the NO oxidation rate, but to an improvement of the proximity between the NO oxidation sites and the NOx storage sites, which is known to be a key factor for a fast NOx storage [33].

3.3. NOx storage-reduction efficiency

In this section, the influence of ceria additions was investigated first in Pt/20Ba/Al reference sample, and secondly in the Mn modified catalyst (Pt/20BaMn/Al, $(Mn/Ba)_{molar\ ratio}$ =1).

3.3.1. NOx storage-reduction efficiency of Pt/20BaCeX/Al catalysts

3.3.1.1. Effect of the cerium loading

The NOx removal efficiency tests in cycling condition were performed at 200, 300 and 400°C in order to study the influence of the Ce loading in Pt/20Ba/Al. The results are reported in Figures 3a, 3b and 3c depending on the temperature test. First, note that the NOx conversion rate is always lower than the NOx storage rate whatever the temperature test. These results indicate that the NOx conversion is not limited by the storage step but by the reduction step. In addition, the introduced hydrogen during the rich pulses in never totally converted. Then, the amount if introduced reducer is not a limiting parameter. However, the H_2 conversion rate is enhanced with the increase of the ceria loading. This was expected since ceria is easily reduced in rich atmosphere.

At 200°C, the influence of the ceria loading is not really significant compared with Pt/20Ba/Al (Figure 3a). The maximum NOx conversion is obtained with Pt/20BaCe1/Al catalyst at 38%, compared with 35% for the sample without ceria. The ammonia selectivity is always higher with the Ce-modified catalysts, between 27 and 35% versus 22% for Pt/20Ba/Al. Finally,

among the modified samples, the optimal Ce loading is obtained with $(Ce/Ba)_{molar\ ratio}$ =1. Pt/20BaCe1/Al exhibits both the higher NOx conversion and the lower ammonia selectivity, even though Pt/20BaCe1/Al catalytic behaviors are still close to those obtained with the Pt/20Ba/Al reference catalyst. Besides, it should be remembered that modification with Mn or Fe led to a catalyst deactivation at this temperature at 200°C [11].

The influence of cerium addition is more significant at higher temperatures. At 300 and 400°C (Figure 3b and 3c), Ce addition always improves the NOx conversion compare with Pt/20Ba/Al. An optimal rate is obtained with Pt/20BaCe1/Al again. At 300°C, the NOx conversion reaches 50%, versus 29 % for Pt/20Ba/Al. At 400°C, the corresponding rates are 63 and 45%, respectively. For higher Ce loadings, the NOx conversion decreases. It can be attributed to the significant surface area losses, as previously discussed in section 3.2. Interestingly, at 300 and 400°C, the ammonia selectivity continuously decreases with the ceria loading, whatever the NOx conversion rates. At 300°C, the ammonia selectivity is a little higher with $(Ce/Ba)_{molar\ ratio}$ = 0.25 compared with Pt/20Ba/Al (25% versus 21%), but it decreases from 25 to 8% with the increase of the cerium loading until $(Ce/Ba)_{molar\ ratio}$ = 2. At 400°C, the ammonia selectivity is always lower with the Ce-containing catalysts. It varies between 22 and 4% for Pt/20BaCe0.25/Al and Pt/20BaCe2/Al, respectively.

These results are consistent with those obtained previously with $Pt/Ce_xZr_{1-x}O_2$ catalysts [30]. It was demonstrated that the ammonia selectivity obtained in similar condition test was dependant of the ceria-zirconia composition. The more the support composition was cerium loaded; the lower was the ammonia selectivity.

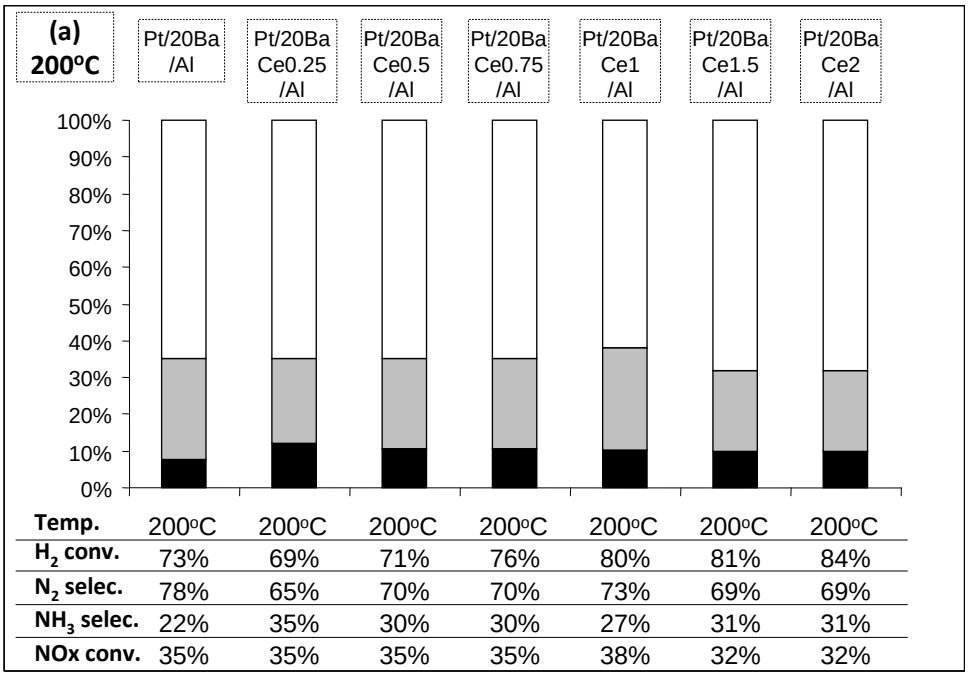

Temp.	200°C	200°C	200°C	200°C	200°C	200°C	200°C
H_2 conv.	73%	69%	71%	76%	80%	81%	84%
N_2 selec.	78%	65%	70%	70%	73%	69%	69%
NH_3 selec.	22%	35%	30%	30%	27%	31%	31%
NOx conv.	35%	35%	35%	35%	38%	32%	32%

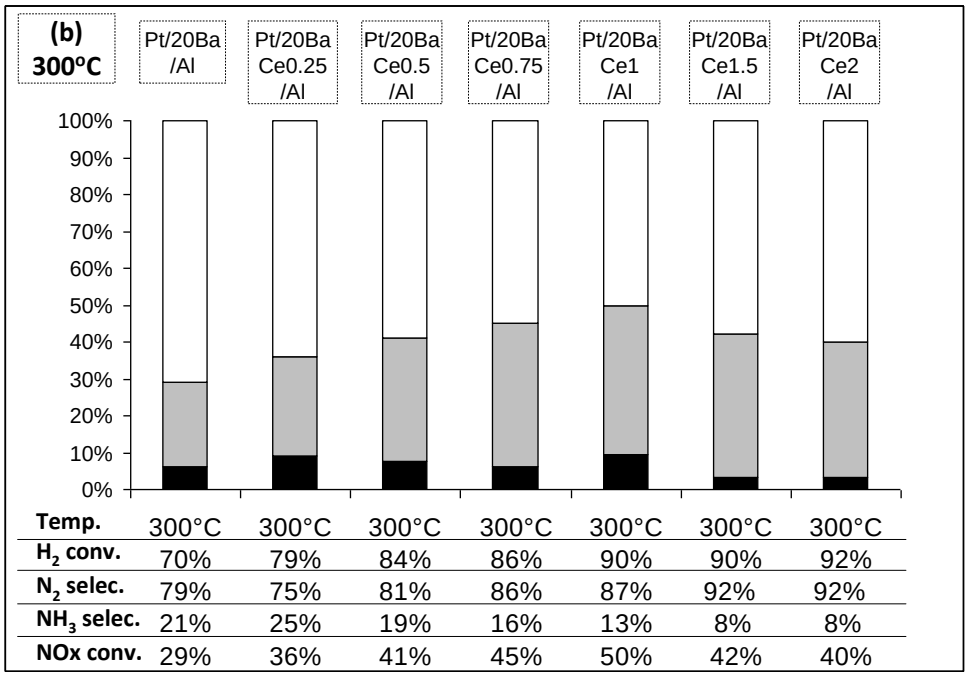

Temp.	300°C	300°C	300°C	300°C	300°C	300°C	300°C
H_2 conv.	70%	79%	84%	86%	90%	90%	92%
N_2 selec.	79%	75%	81%	86%	87%	92%	92%
NH_3 selec.	21%	25%	19%	16%	13%	8%	8%
NOx conv.	29%	36%	41%	45%	50%	42%	40%

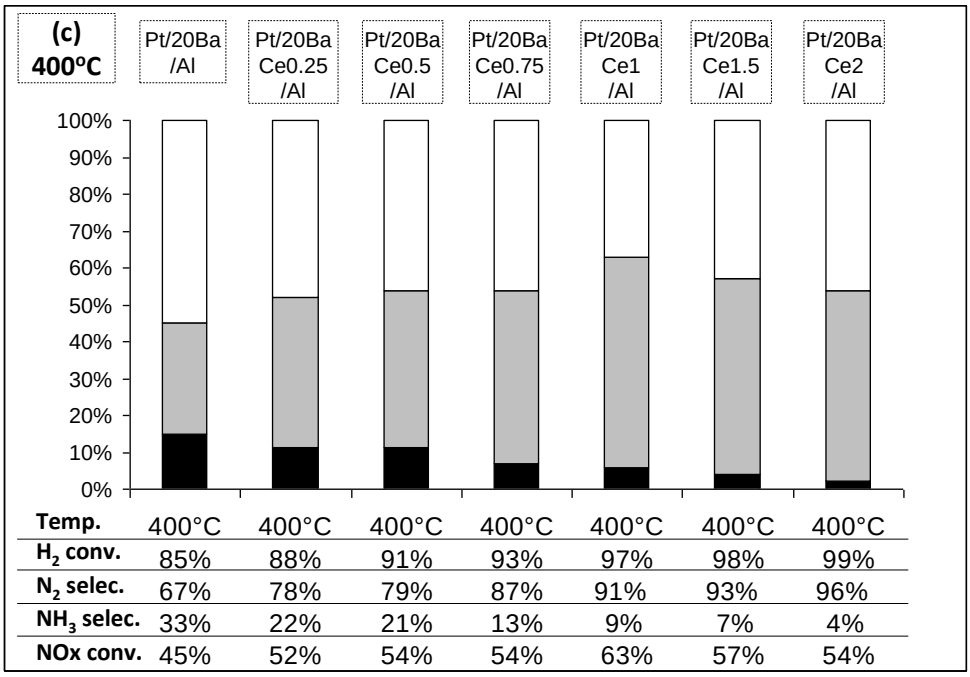

Temp.	400°C	400°C	400°C	400°C	400°C	400°C	400°C
H_2 conv.	85%	88%	91%	93%	97%	98%	99%
N_2 selec.	67%	78%	79%	87%	91%	93%	96%
NH_3 selec.	33%	22%	21%	13%	9%	7%	4%
NOx conv.	45%	52%	54%	54%	63%	57%	54%

Figure 3: Influence of the cerium loading in Pt/20BaCeX/Al catalyst: NOx storage/reduction efficiency test at 200 (a), 300 (b) and 400°C (c) with 3% H_2 in the rich pulses. NOx conversion (%) into N_2 (□) and into NH_3 (■) and related data.

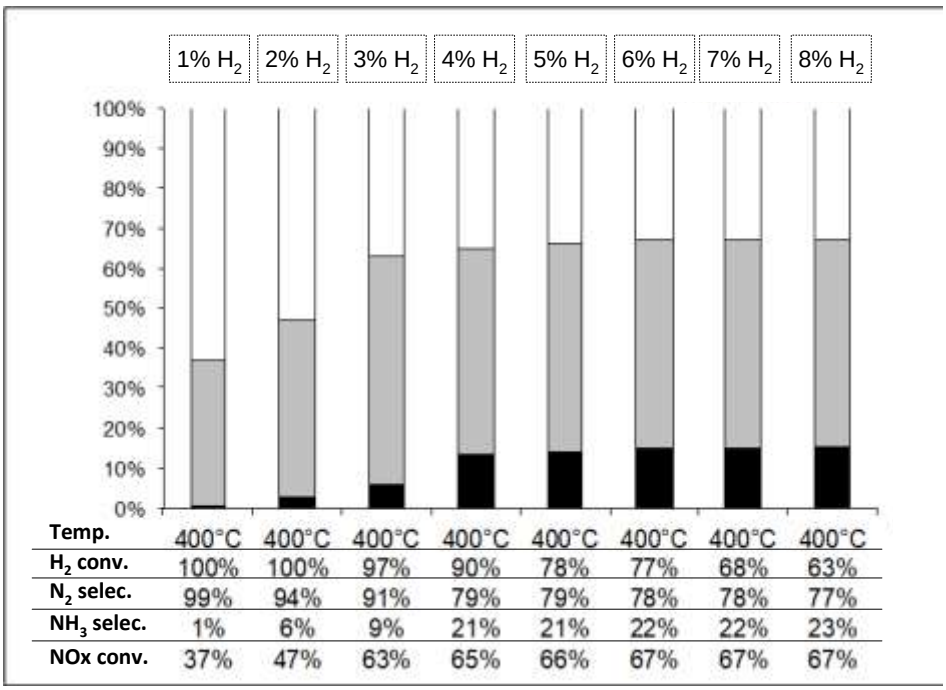

Temp.	400°C	400°C	400°C	400°C	400°C	400°C	400°C	400°C
H_2 conv.	100%	100%	97%	90%	78%	77%	68%	63%
N_2 selec.	99%	94%	91%	79%	79%	78%	78%	77%
NH_3 selec.	1%	6%	9%	21%	21%	22%	22%	23%
NOx conv.	37%	47%	63%	65%	66%	67%	67%	67%

Figure 4: Pt/20BaCe/Al catalyst. NOx storage/reduction efficiency test at 400°C. NOx conversion (%) into N_2 (□) and into NH_3 (■) and related data. Influence of H_2 concentration in the rich pulses (1-8%).

3.3.1.2. Effect of H_2 concentration in the rich pulses

Then, cerium addition dramatically decreases ammonia emission, even if the introduced hydrogen is not fully converted. In order to check this point, additional measurements were carried out at 400°C with Pt/20BaCe1/Al. The H_2 concentration in the rich pulses was varied between 1 and 8%. Results are reported in Figure 4. With 1%H_2, the NOx conversion is limited at 37 %, the introduced reducer is totally converted and there is nearly no ammonia emission. The increase of the hydrogen concentration up to 2% leads to a significant improvement of the NOx conversion, at 47%. H_2 is still totally converted and the ammonia selectivity is still low, at 6%. 3%H_2 is a transitional concentration. The NOx conversion increases again, at 63%, few hydrogen remains (97% are converted) and ammonia selectivity becomes significant, at 9%. From 4 to 8% H_2, the NOx conversion is rather constant at 65-67%. In opposition with results obtained with Pt/20Ba/Al and Pt/20BaMn/Al [11], the ammonia selectivity becomes almost constant at 21-23%, despite the increase of the hydrogen concentration. Then, it confirms the beneficial effect of Ce addition on the ammonia selectivity, even in the case of a large hydrogen excess.

3.3.1.3. Conclusion about the cerium influence

Finally, Ce addition leads to a noteworthy NOx conversion improvement at 300 and 400°C which can be attributed to an improvement of the NOx reduction by ammonia formed in-situ. A slight improvement can be obtained at 200°C, depending on the ceria loading. For comparison, Mn addition leads to similar NOx conversion improvement at 400°C, but also to a deactivation of the catalyst at 200°C and 300°C. However, the remarkable behavior of the Pt/20BaCeX/Al catalysts is to limit the ammonia selectivity, with a positive effect of the cerium loading. Nevertheless, for the higher cerium content, the BET surface area drop induces a lower NOx conversion rate. Then the optimal $(Ce/Ba)_{molar\ ratio}$ was found to be 1. With this Pt/20BaCe1/Al catalyst, the ammonia selectivity reaches a limited rate of approximately 22-23% at 400°C if a large hydrogen excess is introduced during the rich pulses, whereas Pt/20Ba/Al and Pt/20BaMn/Al catalysts exhibited ammonia selectivity until 40% with the same experimental conditions.

Further investigations were done with the aim to combine the beneficial effects of cerium and manganese additions. Pt/20BaMn/Al formulation was selected and it was modified by ceria addition. A part of alumina was then replaced in order to obtain four (Ce/Ba) molar ratios between 0.1 and 1.

3.3.2. NOx storage-reduction efficiency of Pt/20BaMnCeX/Al catalysts

The influence of cerium addition on the NOx storage-reduction efficiency of Pt/20Mn/Al was studied at 200, 300 and 400°C using first 3% H_2 in the rich pulses. For comparison, results obtained with the Pt/20Ba/Al reference catalyst are also reported in Figures 5 and 6, depending on the temperature test.

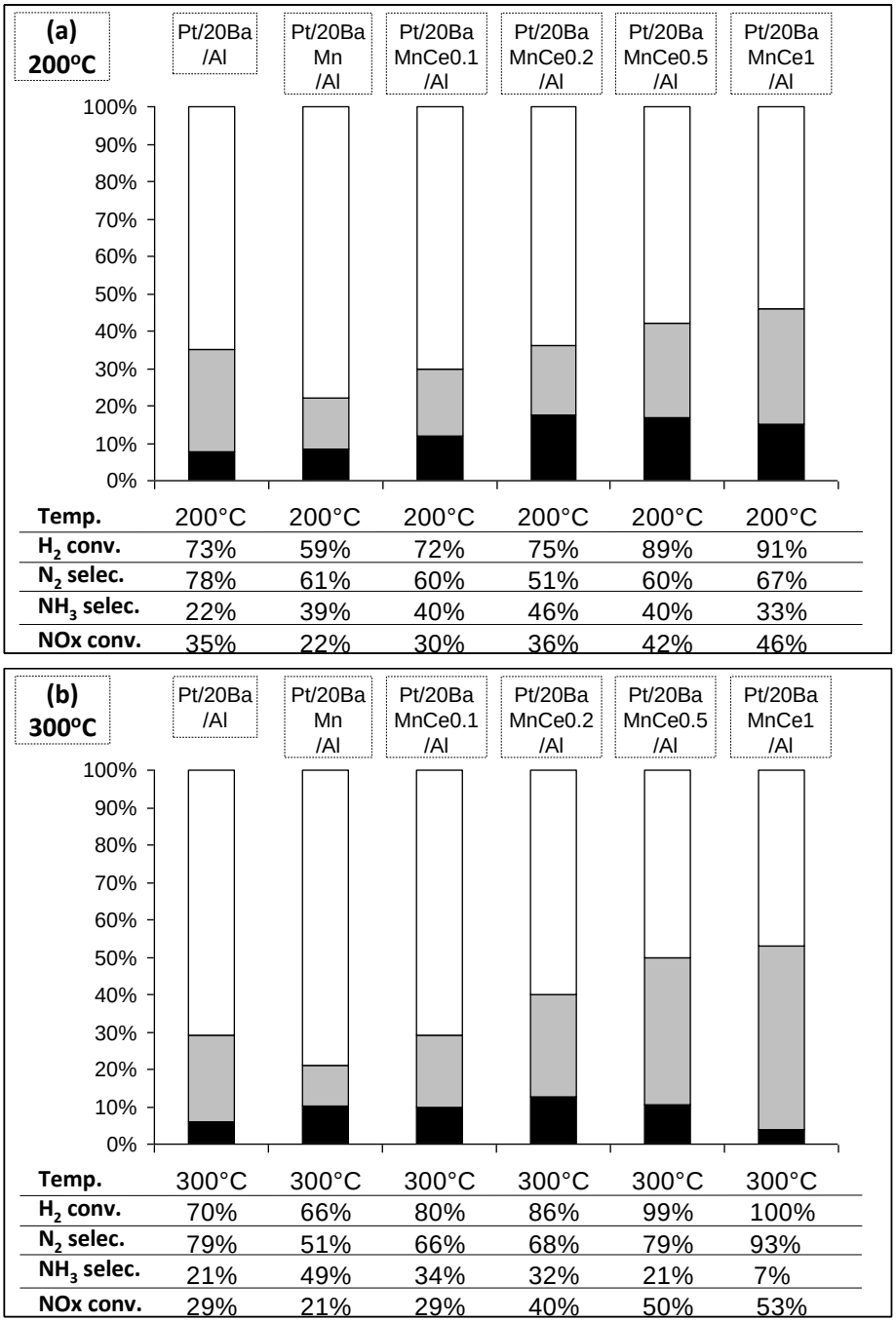

Figure 5: Influence of the cerium loading in Pt/20BaMnCeX/Al catalyst: NOx storage/reduction efficiency test at 200 (a) and 300°C (b) with 3% H_2 in the rich pulses. NOx conversion (%) into N_2 (□) and into NH_3 (■) and related data.

At 200 and 300°C (Figures 5a and 5b), the NOx conversion is always lower than the NOx storage rate (Table 3), indicating that the whole process is limited by the reduction step again at these temperatures.

At 200°C, it was already reported that Mn addition led to a catalyst deactivation. Addition of cerium allows a continuous increase of the NOx conversion which becomes higher than the conversion obtained with the Pt/20Ba/Al reference catalyst for $(Ce/Ba)_{molar\ ratio} \geq 0.2$. Ammonia selectivity remains high at low cerium content (around 40%). It decreases at high cerium loading (33% for Pt/20BaMnCe1/Al), even if the selectivity remains higher than the value obtained with Pt/20Ba/Al, at 22%.

Compared with results obtained at 200°C, the NOx conversion at 300°C increases more significantly with the cerium loading, from 22% for Pt/20BaMn/Al to 53% for Pt/20BaMnCe1/Al. $(Ce/Ba)_{molar\ ratio} = 0.1$ is enough to observe similar NOx conversion than Pt/20Ba/Al. The influence of the cerium loading on the ammonia selectivity is more significant at 300°C compared with results at 200°C. The ammonia selectivity continuously decreases, down to 7% for Pt/20BaMnCe1/Al. However, with this catalyst, the introduced hydrogen is fully converted, which is favorable for low ammonia emission. The influence of the hydrogen concentration on the NOx conversion and selectivity is examined in a next part below.

At 400°C with 3% H_2 in the rich pulses, the hydrogen conversion reaches 100% with all the modified catalysts (Figure 6a). As a consequence, the NOx conversion could be limited by the reducer amount. However, it was previously found that manganese addition improves the NOx conversion and the selectivity of Pt/20Ba/Al catalyst at this temperature. Further cerium additions improve again the deNOx activity, and a maximum NOx conversion rate of 76% is observed with Pt/20BaMnCe0.5/Al. In the same time, the ammonia selectivity, which was already low with Pt/20BaMn/Al (7%) becomes nil from $(Ce/Ba)_{molar\ ratio} = 0.5$ in Pt/20BaMnCeX/Al catalysts. Thus, with this condition with full H_2 conversion, the in-situ formed ammonia is able to react with the remaining stored NOx to produce N_2, with a promoting effect of the cerium loading.

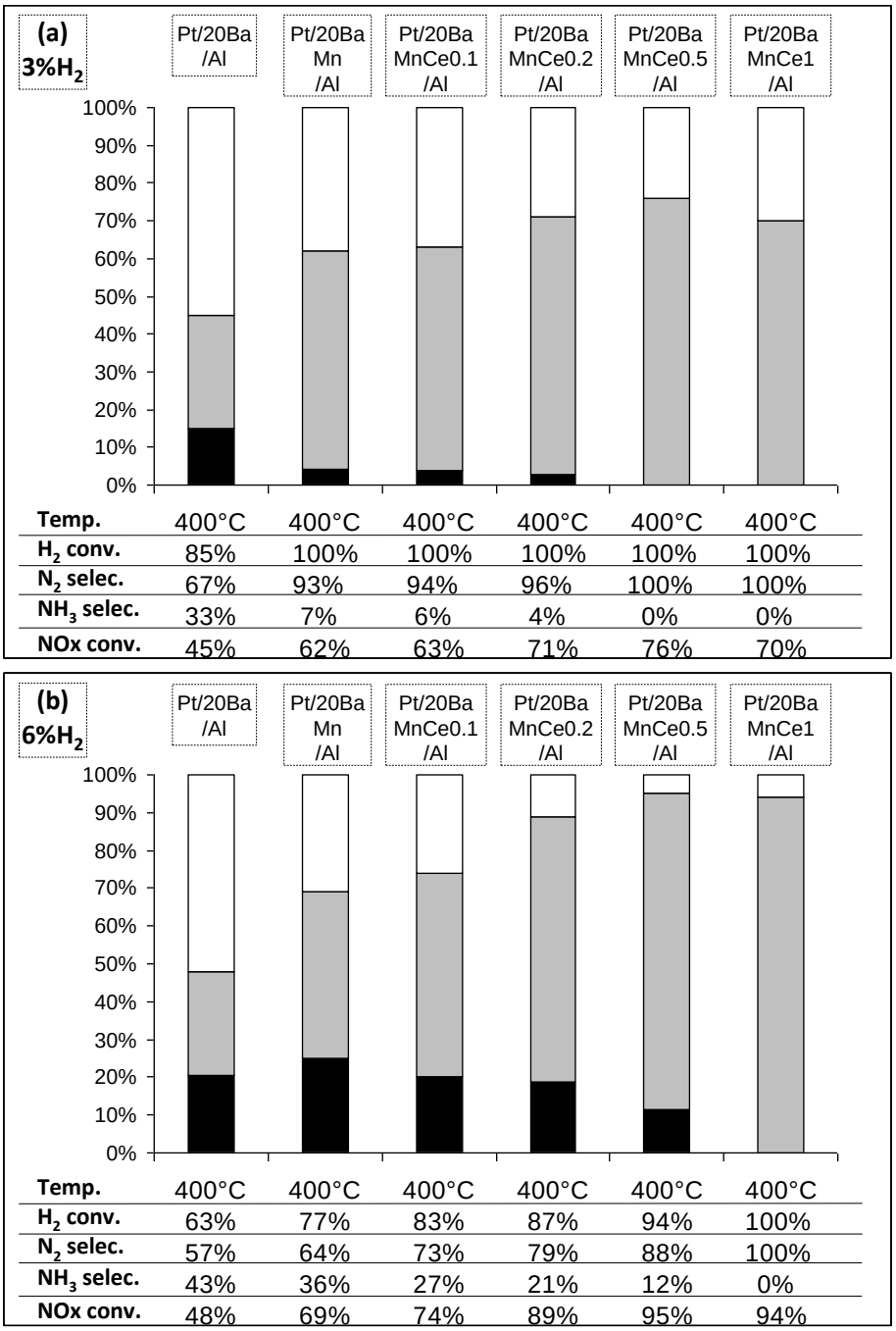

Figure 6: Influence of the cerium loading in Pt/20BaMnCeX/Al catalyst: NOx storage/reduction efficiency test at 400°C with 3% H_2 (a) or 6% H_2 (b) in the rich pulses. NOx conversion (%) into N_2 (□) and into NH_3 (■) and related data.

With the higher cerium loading (Pt/20BaMnCe1/Al), the NOx conversion reaches only 70%, even if this sample exhibits the higher NOx storage rate, at 99% for 60s. This result can be attributed to the important hydrogen consumption due to the catalyst reduction and the NOx NOx conversion could be limited by the reducer amount. Then, supplementary tests were performed with higher H_2 concentration in the rich pulses (6%), with the aim to have no limitation by the reducer amount.

With 6% H_2 in the rich pulses (Figure 6b), the hydrogen consumption is total only with Pt/20BaMnCe1/Al and the influence of the cerium loading is more pronounced. A significant NOx conversion improvement is observed with the cerium content, from 69% with Pt/20BaMn/Al to 94-95% with the two catalysts with the higher cerium loading. These values can be considered as optimal values since the NOx storage rates of these two samples reach 96-99%, and because a NOx desorption without reduction is usually observed during the process [34]. In addition with the NOx conversion improvement, the ammonia selectivity clearly decreases with the cerium loading. It suggests that cerium promotes the reaction between ammonia and stored NOx, even if the introduced hydrogen is not totally converted.

For a better understanding of the Mn-Ce modified catalysts behaviors, tests with various H_2 concentrations were performed at 300 and 400°C. Pt/20BaMnCe0.5/Al was selected because Pt/20BaMnCe1/Al exhibits very high H_2 consumption.

At 300°C (Figure 7a), the NOx conversion increases from 24 to 54% with the increase of the H_2 concentration in the rich pulses from 1 to 4%. Higher hydrogen concentration does not improve the NOx conversion rate anymore. In opposition, the ammonia selectivity is limited to 21-23 % when H_2 is fully converted, and it increases until 34% with 6% H_2 in the rich pulses. Thus, at 300°C, ammonia is always detected even if the introduced H_2 is fully converted. It means that the reaction rate between the in-situ formed ammonia and the stored NOx is lower compared with the ammonia formation rate, i.e. NOx react preferentially with H_2 to form ammonia than with ammonia itself to form N_2 at this temperature.

At 400°C (Figure 7b), the NOx conversion rate increases with the hydrogen concentration until it reaches 95% with 6% H_2, which can be considered as a maximum conversion value. Since the introduced hydrogen is fully converted, no ammonia emission is observed, in opposition with results obtained at 300°C, indicating that the ammonia reactivity is significantly improved at 400°C. H_2 remains for introduced concentration of 5% and higher, and ammonia is then detected. However, the ammonia selectivity is limited to 16-17% from 7% H_2 in the rich pulses. Then, the beneficial effect of cerium addition on the maximum ammonia selectivity is observed again, as seen in section 3.3.1 with Pt/20BaCe1/Al catalyst. Moreover, the NOx conversion is improved when Mn and Ce are added together.

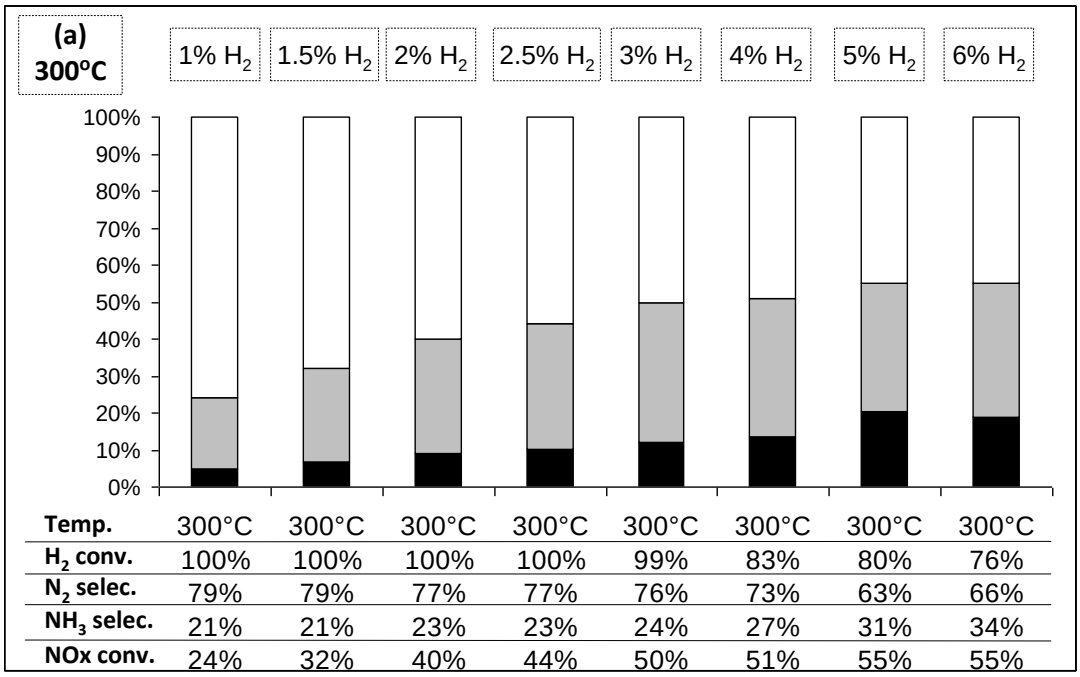

Temp.	300°C	300°C	300°C	300°C	300°C	300°C	300°C	300°C
H_2 conv.	100%	100%	100%	100%	99%	83%	80%	76%
N_2 selec.	79%	79%	77%	77%	76%	73%	63%	66%
NH_3 selec.	21%	21%	23%	23%	24%	27%	31%	34%
NOx conv.	24%	32%	40%	44%	50%	51%	55%	55%

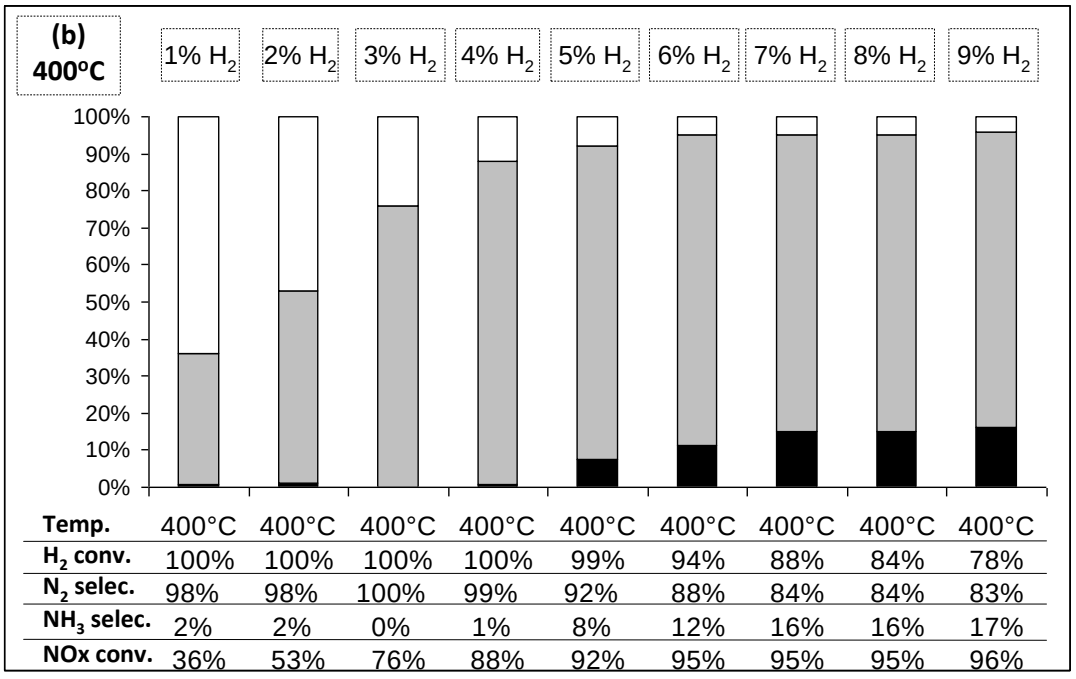

Temp.	400°C	400°C	400°C	400°C	400°C	400°C	400°C	400°C	400°C
H_2 conv.	100%	100%	100%	100%	99%	94%	88%	84%	78%
N_2 selec.	98%	98%	100%	99%	92%	88%	84%	84%	83%
NH_3 selec.	2%	2%	0%	1%	8%	12%	16%	16%	17%
NOx conv.	36%	53%	76%	88%	92%	95%	95%	95%	96%

Figure 7: Pt/20BaMnCe0.5/Al catalyst (60mg): NOx storage/reduction efficiency test at 300 (a) and 400°C (b). NOx conversion (%) into N_2 (□) and into NH_3 (■) and related data. Influence of H_2 concentration in the rich pulses.

3.3.3. Conclusion on the influence of the Mn, Ce and Mn-Ce additive on the NSR behavior

Finally, Ce addition in Pt/20Ba/Al leads to slight improvement of the NOx conversion at 200°C. The enhancement of the catalytic properties is more significant at higher temperature, and

especially at 400°C. It can be attributed to an improvement of the reaction between the ammonia formed in-situ and the remaining stored NOx.

At 200 and 300°C, cerium addition compensates the inhibiting effect of Mn addition previously observed with Pt/20BaMn/Al catalyst, especially with the higher cerium loading. At 400°C, high NOx conversions can be obtained, near 100%, with very low ammonia emission. Comparison of the NSR behaviors at 400°C of Pt/20Ba/Al, Pt/20BaMn/Al, Pt/20BaCe1/Al and Pt/20BaMnCe0.5/Al catalysts is reported in Figure 8. It shows that Pt/20BaMnCeX/Al catalysts exhibit the beneficial effects of both Mn and Ce for the NOx conversion. Moreover, it also puts in evidence that addition of cerium in Pt/20Ba/Al and in Pt/20BaMn/Al leads to a limitation of the maximum ammonia selectivity at a low level compared with Pt/20Ba(Mn)/Al catalysts. The ammonia selectivity tends to 40% with Pt/20Ba/Al and Pt/20BMn/Al, and it is two times lower with the Ce-containing catalysts.

Ji et al. [35] have showed somewhat similar results. They have tested catalysts with various ceria contents and they have observed that the ammonia selectivity decreased with the increase of the ceria loading. They have proposed that ammonia could react with the available oxygen from the ceria surface. Then, the reducibility of the samples were studied, using H_2 temperature programmed reduction (TPR) and oxygen storage capacity (OSC) measurements.

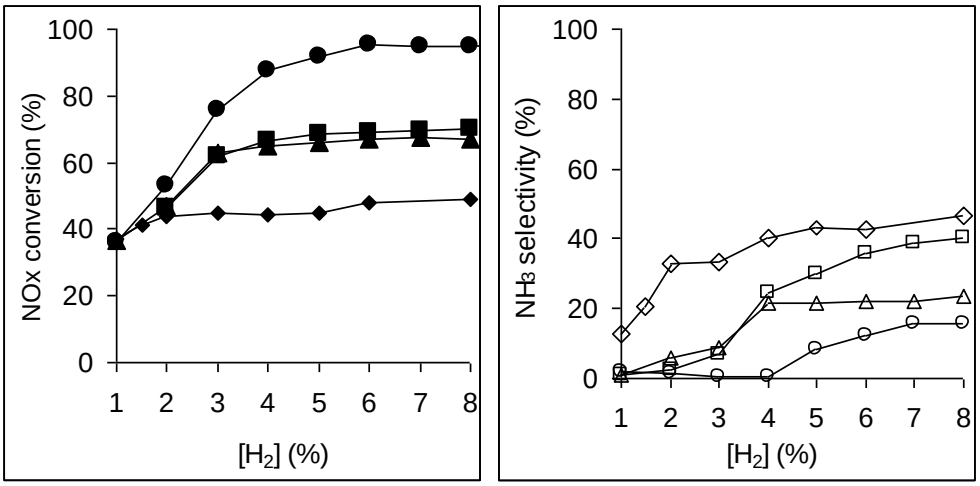

Figure 8: NOx conversion rate (full symbols) and NH_3 selectivity (open symbols) measured at 400°C depending on hydrogen concentration in the rich pulses for Pt/20Ba/Al (◆,◇), Pt/20BaMn/Al (■,□), Pt/20BaCe1/Al (▲,△) and Pt/20BaMnCe0.5/Al (●,○).

3.4. Role of the catalyst reducibility

3.4.1. TPR measurements

First, it was previously showed that Pt/Ba/Al catalyst did not exhibit significant H_2 consumption using the same TPR operating condition [23]. In addition, whatever the studied catalyst, no significant H_2 consumption was observed below 100°C.

The TPR profiles of the Pt/20BaMnCeX/Al catalysts are reported in Figure 9.

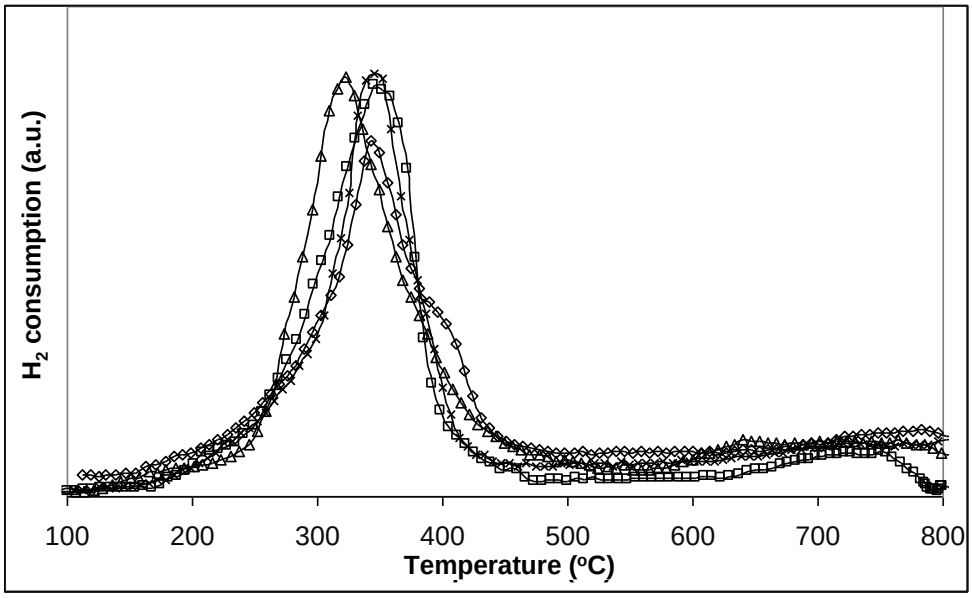

Figure 9: H_2-TPR profiles of Pt/20BaMn/Al (△), Pt/20BaMnCe0.2/Al (□), Pt/20BaMnCe0.5/Al (◇) and Pt/20BaMnCe1/Al (×) catalysts.

The reduction of 20BaMn/Al material without platinum was also studied. Its reduction profile (not shown) exhibits H_2 consumption in the 100-800 temperature range, with a main peak near 550-600°C and two broad peaks near 300 and 750°C. These temperatures are higher than those reported by Christel et al. [36] for the reduction of unsupported MnO_2 ($2MnO_2 + H_2 \rightarrow Mn_2O_3 + H_2O$ near 250°C, $3Mn_2O_3 + H_2 \rightarrow 2Mn_3O_4 + H_2O$ at 280°C, and $Mn_3O_4 + H_2 \rightarrow 3MnO + H_2O$ near 450°C). This stabilization of the manganese oxide can be attributed to interactions with other compounds such as barium, leading for instance to $BaMnO_3$ as detected by XRD (see section 3.1.). The Pt/20BaMn/Al sample (symbol (△) in Figure 9) exhibits one main peak in the 250-450°C temperature range and a small H_2 consumption in the 600-800°C temperature range. Then, platinum dramatically favors the manganese reduction, probably due to the hydrogen activation. In addition, this result indicates that platinum and manganese are close together. Assuming that manganese is reduced into Mn^{II} at the end of the TPR test (after 30 min

at 800°C), H_2 consumption quantification allows the evaluation of the initial manganese mean redox state according $MnO_x + (x-1)\ H_2 \rightarrow MnO + (x-1)\ H_2O$. The obtained manganese redox state is 3.2, indicating that Mn^{III} species such as Mn_2O_3 are predominant, with also the presence of Mn^{IV} ($BaMnO_3$, MnO_2).

Compared with Mn containing samples, 20BaCe/Al and Pt/20BaCe/Al samples tested with the same protocol exhibit very low hydrogen consumption (results not shown). However, the typical two steps reduction of CeO_2 was obtained. The reduction of the Ce^{IV} surface species occurs first (at about 300°C without platinum, and near 200°C when the promoting effect of platinum is observed). The reduction of bulk ceria is obtained for higher temperature, it is not achieved at 800°C [37,38].

The influence of Ce loading on the TPR profiles of Pt/20BaMnCeX/Al samples is also reported in Figure 9. In fact, cerium addition induces only small changes. The total H_2 consumption is not really affected by the ceria addition; only a small shift of the main manganese reduction peak is noticeable, from 320 to 340°C.

Finally, the TPR measurements do not allow us to obtain a correlation between the samples reducibility and the catalytic activity in cycling condition. Ceria loading induces significant improvement in NSR measurements but the reducibility evaluated by H_2-TPR is mainly dependant of the presence of manganese. However, catalytic tests were performed in cycling condition, in opposition with the TPR measurements. Then, further investigations were performed to evaluate the reducibility of the catalysts in cycling conditions.

3.4.2. OSC measurements

OSC measurements were performed at 400°C using the CO-O_2 pulsed method. Results obtained for Pt/20Ba/Al, Pt/20BaMn/Al, Pt/20BaCe/Al and Pt/20BaMnCe1/Al and catalysts are reported in Table 4.

The Pt/20Ba/Al reference catalyst exhibits an OSC value of 28 $\mu mol_O\ g^{-1}$. Addition of manganese leads to a two times higher OSC whereas TPR experiments show a high reducibility. In opposition with the TPR results, catalyst modified by ceria addition presents redox properties in cycling condition significantly higher than Pt/20BaMn/Al, with 121 $\mu mol_O\ g^{-1}$ versus 61 $\mu mol_O\ g^{-1}$, respectively. TPR experiments also showed that the reducibility of Pt/20BaMnCeX/Al samples was not significantly affected by ceria addition. On the contrary, the OSC of Pt/20BaMn/Al is more than three times enhanced after Ce addition (Pt/20BaMnCe1/Al catalyst, Table 4). Then, compared with manganese addition, ceria addition

largely improves the available oxygen on the catalyst surface in transient condition, with a synergetic effect of the simultaneous presence of manganese and cerium.

Table 4: Oxygen storage capacities (OSC, $\mu mol_O.g^{-1}$) measured at 400°C for Pt/20Ba/Al, Pt/20BaMn/Al, Pt/20BaCe/Al et Pt/20BaMnCe1/Al catalysts.

Catalyst	Pt/20Ba/Al	Pt/20BaMn/Al	Pt/20BaCe/Al	Pt/20BaMnCe1/Al
OSC ($\mu mol_O\ g^{-1}$)	28	61	121	403

3.4.3. Discussion

In the first part of this study [11], it was demonstrated that ammonia is one of the intermediate in the NOx reduction process. With Pt/20Ba/Al catalysts, ammonia emission is due to the fact that the ammonia formation rate, via the NOx+H_2 reaction, is lower than the reaction rate between this in-situ formed ammonia and the stored NOx in order to obtain N_2. At 400°C, there is no ammonia emission if the introduced hydrogen is fully converted. This general trend is always observed whatever the composition of the studied catalysts, but only at 400°C (Figure 7). In accordance with the OSC measurements, the higher is the OSC, the higher is the hydrogen consumption and ammonia is emitted for higher hydrogen concentration. For temperature below 400°C, ammonia can be observed even if hydrogen is fully converted (Figure 7). It indicates that NOx+NH_3 reaction rate remains limited, even with the more active catalysts for this reaction. When H_2 is not fully converted, examination of the obtained results indicates some correlation between the amount of remaining hydrogen and the ammonia selectivity, but there is a large dispersion of the points depending on the catalyst composition and the catalytic test condition (figure not shown).

Mn addition to Pt/20Ba/Al can induce a significant improvement of the NOx conversion, but only at 400°C. It was attributed to an enhancement of the NOx reduction with ammonia. Ceria also improves the NOx reduction with ammonia (Figures 3 and 6), from 300°C. Contrary to manganese, ceria clearly leads to lower ammonia emission, even if the introduced hydrogen is not fully converted (large H_2 excess, Figure 8). Then, the available oxygen from ceria is supposed to participate to the ammonia oxidation. Two products can be considerate, N_2 and/or NOx, both leading to lower ammonia selectivity. Figure 8 shows that, for high hydrogen concentration, Pt/20BaCe/Al exhibits similar NOx conversion compared with Pt/20BaMn/Al, both catalysts being more efficient than Pt/20Ba/Al. However, the ammonia selectivity is

significantly lower and limited with the ceria containing catalysts (Ce and Mn-Ce modified catalysts). As a consequence, the main product of the ammonia oxidation by the available oxygen from the support should be N_2 since oxidation into NOx should decrease the NOx conversion. Finally, ceria promotes both the NOx+NH_3 reaction, from 300°C, and the ammonia oxidation into N_2 via the available oxygen at the catalyst surface. A synergetic effect is observed when the catalyst contains both Ce and Mn: OSC is largely enhanced and, at the same time, NOx conversion and ammonia emission are improved. Nearly total NOx conversion into N_2 can be obtained (Figure 6) at 400°C, which indicates high NOx reduction rates (NOx reduction into NH_3 and then NH_3 reaction with stored NOx or oxygen in order to obtain N_2). However, the NOx reduction efficiency at 300°C is still limited, notably due to insufficient NOx+NH_3 reaction rate (ammonia emission even in the case of total H_2 conversion).

In addition to the improvement of the reaction between NH_3 and the stored NOx with the increase of the ceria loading, two other phenomenons can be considered.

Firstly, the increase of the H_2 consumption with the increase of the ceria loading indicates that a part of the support is also reduced during the rich pulses, in accordance with the OSC measurements carried out in cycling condition. Then, the NO decomposition over the reduced ceria can be considered [39]. Nevertheless, such a reaction should not induce a decrease of the ammonia yield, as observed for example in Figure 3c.

However, the increase of the H_2 consumption with the ceria loading also leads to a lower H_2 pressure at the end of the catalytic bed. Then, a lower NH_3 selectivity could be expected in the tail of the catalytic bed, which would be compatible with the observed results. Two points allow us to decline this hypothesis. First, whatever the studied catalyst, no ammonia emission is observed only in the case of total H_2 conversion, and only at 400°C. Secondly, at 300°C, the ammonia selectivity reaches around 20% even if the introduced hydrogen is fully converted (figure 7a, Pt/20BaMnCe0.5/Al catalyst), but the beneficial effect of the cerium loading on both NOx conversion and ammonia selectivity is observed (figure 5b and 3b). Then, the decrease of the ammonia yield in presence of remaining H_2 conversely with the increase of the N_2 yield suggests that the reaction between NH_3 and the stored NOx is the main cause of the NOx reduction improvement. The NO decomposition over reduced ceria can not be excluded, but it seems to be negligible.

Nevertheless, the activity improvement obtained by cerium addition should be not attributed only to its OSC properties. Indeed, in a recent study, Pt/$Ce_xZr_{1-x}O_2$ catalysts were studied [30]. The increase of the cerium content led to an increase of the NOx conversion and,

simultaneously, to a decrease of the ammonia selectivity (i.e. improvement of the $NOx+NH_3$ reaction). Among the studied composition, the best activity was obtained with $Pt/Ce_{0.8}Zr_{0.2}O_2$, which exhibited the higher cerium content, whereas $Pt/Ce_{0.58}Zr_{0.42}O_2$ exhibited the higher OSC.

4. Conclusion:

In the first part of this study, it was shown that Mn addition to Pt/20Ba/Al led to an improvement of the NOx reduction (conversion and selectivity), but only at 400°C, whereas the activity was inhibited at 200 and 300°C. With ceria modified Pt/20Ba/Al catalyst, no deactivation is observed at 200°C and significant improvements were obtained from 300°C. In addition to the enhancement of the $NOx+NH_3$ reaction, ceria addition led to a limitation of the ammonia selectivity at a lower level compared with Pt/20Ba(Mn)/Al catalysts. It was attributed to the ammonia oxidation into N_2 via the available oxygen at the catalyst surface. A synergetic effect was observed between Mn and Ce in Pt/20BaMnCeX/Al catalysts. A near total NOx conversion can be observed at 400°C, and ammonia is limited to a lower level. These results are correlated with a large improvement of the oxygen mobility for the Mn-Ce containing catalysts, even if this parameter should be not the only one.

Al lower temperature (300°C), the reduction rates are still the limiting steps of the NSR process, notably because of the insufficient $NOx+NH_3$ reaction rate.

Refrerences

[1] W.S. Epling, L.E. Campbell, A. Yezeerets, N.W. Currier, J.E. Parks II, Catal. Rev. 46 (2004) 163-245.
[2]T. Kobayashi, T. Yamada, K. Kayano, SAE Technical Papers 970745 (1997) 63.
[3] S. Matsumoto, Cattech 4 (2000) 102-109.
[4] C. Sedlmair, K. Seshan, A. Jentys, J.A. Lercher, Catal. Today 75 (2002) 413-419.
[5] E.C. Corbos, X. Courtois, N. Bion, P. Marecot, D. Duprez, Appl. Catal. B 80 (2008) 62–71.
[6] J. Li, J. Theis, W. Chun, C. Goralski, R. Kudla, J. Ura, W. Watkins, M. Chattha, R. Hurley, SAE Technical Paper no 2001-01-2503 (2001).
[7] D. Uy, A.E. O'Neill, J. Li and W.L.H. Watkins, Top. Catal. 95 (2004) 191-201.
[8] M. Casapu, J.D. Grunwaldt, M. Maciejewski, M. Wittrock, U. Göbel and A. Baiker, Appl. Catal. B 63 (2006) 232-242.
[9] R.D. Clayton, M.P. Harold, V. Balakotaiah, Appl. Catal. B 84 (2008) 616-630.
[10] L. Lietti, I. Nova, P. Forzatti, J. Catal. 257 (2008) 270-282.
[11] N. Le Phuc, X. Courtois, F. Can, S.Berland, S. Royer, P. Marecot, D. Duprez, submitted in Appl. Catal. B.

[12] K. Yamazaki, T. Suzuki, N. Takahasi, K. Yojota, M. Sugiura, Appl. Catal. B 30 (2001) 459-468.
[13] P. T. Fanson, M.R. Horton, W.N. Delgass, J. Lauterbach, Appl. Catal. B 46 (2003) 393-413.
[14] J. Huang, Z. Tong, Y. Huang, J. Zhang, Appl. Catal B 78 (2008) 309-314.
[15] U. Bentrup, A. Bruckner, M. Richter, R. Fricke, Appl. Catal. B 32 (2001) 229-241.
[16] J. Xiao, X. Li, S. Deng, F. Wang, L. Wang, Catal. Commun. 9 (2008) 563-567.
[17] X. Liang, J. Li, Q. Lin, K. Sun, Catal. Comm. 8 (2007) 1901-1904.
[18] Z. Wu, B. Jiang, Y. Liu, Appl. Catal. B 79 (2008) 347-355.
[19] F. Dong,A. Suda, T. Tanabe, Y.Nagai, H. Sobukawa, H. Shinjoh, M. Sugiura, C. Descorme, D. Duprez, Catal. Today 93–95 (2004) 827–832.
[20] M. Eberhardt, R. Riedel, U. Göbel, J. Theis, E. S. Lox, Topics Catal. 30/31 (2004) 135-142.
[21] L. F. Liotta, A. Macaluso, G. E. Arena, M. Livi, G. Centi, G. Deganello, Catal. Today 75 (2002) 439-449.
[22] H. Kwak, D.H. Kim, J. Szanyi, C.H.F. Peden, Appl. Catal. B 84 (2008) 545–551.
[23] E.C. Corbos, S. Elbouazzaoui, X. Courtois, N. Bion, P. Marecot, D. Duprez, Topics Catal. 42–43 (2007) 9-13.
[24] H. Mahzoul, L. Limousy, J.F. Brilhac, P. Gilot, J. of Analytical and Applied Pyrolysis 56 (2000) 179-193.
[25] S. Philipp, A. Drochner, J. Kunert, H. Vogel, J. Theis, E. S. Lox, Topics Catal. 30/31 (2004) 235-238.
[26] P. Svedberg, E. Jobson, S. Erkfeldt, B. Andersson, M. Larsson, M. Skoglundh, Topics Catal. 30 (2004) 199-206.
[27] H.Y. Lin, C.J. Wu, Y.W. Chen, C.H. Lee, Ind. Eng. Chem. Res. 45 (2006) 134-141.
[28] M. Machida, D. Kurogi, T. Kijima, Chem. Mater 12 (2000) 3165-3170.
[29] C.N. Costa, A.M. Efstathiou Appl. Catal. B 72 (2007) 240–252.
[30] P.N. Lê, E.C. Corbos, X. Courtois, F. Can, P. Marecot, D. Duprez, Appl. Catal. B 93 (2009) 12-21.
[31] S. Kacimi, J. Barbier Jr., R. Taha, D. Duprez, Catal. Lett. 22 (1993) 343-350.
[32] H. Shinjoh, M. Hatanaka, Y. Nagai, T. Tanabe, N. Takahashi, T. Yoshida, Y.Miyake, Top. Catal. 52 (2009)1967-1971
[33] B. Pereda-Ayo, R. Lopez-Fonseca, J.R. Gonzalez-Velasco, Appl. Catal. A 363 (2009) 73–80
[34] E. Fridell, M. Skoglundh, B. Westerberg, S. Johansson, G. Smedler, J. Catal., 183 (1999) 196-209.
[35] Y. Ji, J-S. Choi, T. J. Toops, M. Crocker, M. Naseri, Catal. Today., 136 (2008) 146-155.
[36] L. Christel, A. Pierre, D. A.M. Rousset Abel, Thermochimica Acta., 306 (1997) 51-59.
[37] H.C. Yao, Y.F. Yu Yao, J. Catal., 86 (1984) 254-265.
[38] E. Rogemond, R. Fréty, V. Perrichon, M. Primet, S. Salasc, M. Chevrier, C. Gauthier, F. Mathis, J. Catal. 169 (1997) 120-131.
[39] G. Ranga Rao, P. Fornasiero, R. Di Monte, J. Kaspar, G. Vlaic, G. Balducci, S. Meriani, G. Gubitosa, A. Cremona, M. Graziani, J. Catal. 162 (1996) 1-9